Article:
Gordon, Jonny, FAGAN, BRENNEN TAYLOR, FINCH, JONATHAN CEDRIC et al. (2026) Black Death land abandonment drove European diversity losses. Ecology Letters. e70325. ISSN: 1461-023X

https://doi.org/10.1111/ele.70325

Title: Black Death land abandonment drove European diversity losses

Authors: Jonathan D. Gordon[1,2,*], Brennen Fagan[1,3], Jonathan Finch[1,2], Lindsey Gillson[1,4,5], Nicky Milner[1,2], Chris D. Thomas[1,4]

Affiliations:

[1] Leverhulme Centre for Anthropocene Biodiversity, University of York; York, UK.

[2] Department of Archaeology, University of York; York, UK.

[3] Department of Mathematics, University of York; York, UK.

[4] Department of Biology, University of York; York, UK.

[5] Plant Conservation Unit, University of Cape Town, Rondebosch, South Africa

*Corresponding author. Address: LCAB, Berrick Saul Building, Harewood Way, Heslington, York, YO10 5DD.

Emails: jonny.gordon@york.ac.uk, brennen.fagan@york.ac.uk, jonathan.finch@york.ac.uk, nicky.milner@york.ac.uk, lindsey.gillson@york.ac.uk, chris.thomas@york.ac.uk

Running title: Biodiversity losses during the European Black Death

Keywords: abandonment, Anthropocene, biodiversity, conservation, depopulation, Holocene, pandemic, pollen, rewilding, vegetation

Article type: Letter

Abstract words, 150; main words, 4,987; text box words, 0.

Number of references, 90; number of figures, 5; number of tables, 0; number of text boxes, 0.

Data accessibility: Pollen data were obtained from the Neotoma Paleoecological Database (http://www.neotomadb.org) and its constituent databases, in particular the European Pollen Database and the Alpine Pollen Database. All data are freely downloadable and cited in-text. All code used in the analysis, along with input datasets, intermediate data products and outputted model fits (etc.) are open access and available from the Dryad Digital Repository: https://doi.org/10.5061/dryad.z08kprrrr.

Author contributions: Conceptualization: JDG, BF, JF, LG, NM, CDT; Methodology: JDG, BF, LG, NM, CDT; Investigation: JDG, BF; Visualization: JDG; Funding acquisition: CDT; Supervision: LG, NM, CDT; Writing – original draft: JDG; Writing – review & editing: JDG, BF, JF, LG, NM, CDT.

Abstract:

The current prevailing perception is that human impacts on the biological realm have been overwhelmingly negative. Here, we test this narrative by considering the consequences for aspects of floristic diversity of the 'Black Death era' (1300–1400 CE), where one third of Europe's population died within half a decade. Based on evidence from 109 pollen records spanning the Common Era, we find increasing floristic diversity from 0 CE to ~1300 CE as human populations increased, followed by rapid and substantial diversity reductions during the famine- and disease-driven human mortality events of the 'Black Death era'. As human populations recovered following the mortality shock, diversity also recovered. Strikingly, it was landscapes characterised by cereal cultivation that generated both the overall Common Era increases *and* the Black Death era declines in diversity. The highest diversity levels were achieved in human-generated, mosaic landscapes, highlighting the integral role of human action in biodiverse European landscapes.

Main Text

Introduction

Mass appropriation of land for food production is widely considered to be the primary driver of biodiversity decline over the last century (IPBES 2019; Krausmann *et al.* 2013; Newbold *et al.* 2015). Yet, over multi millennial timescales, analyses of continental-scale fossil pollen datasets (that contain information on past plant community composition and diversity) suggest the opposite, with increasing diversity associated with intensifying human footprints across multiple biomes and continents (Gordon *et al.* 2024). While not necessarily incompatible, given the different intensities of farming operations during different time periods, these two sets of observations lead to opposing expectations of the biodiversity consequences of land 'abandonment'. Here, we test these alternatives by considering an historical precedent - the 14th Century in Europe, the 'Black Death era' - a period that encompassed the Great Famine (1315 – 1317 CE) as well as the Black Death (1347 – 1353 CE) itself. Previous work has used the pollen record to identify spatial variation in Black Death mortality (Izdebski *et al.* 2022), but here we use the pollen record to ask a fundamentally different question: what were the consequences of the decline of cultivated lands and the subsequent return of cereal farming activities for European floristic diversity over the Black Death era? The answer to this question may inform ongoing conservation choices in Europe, specifically the likely longer-term consequences of 'traditional management' versus 'rewilding' conservation strategies.

The 14th Century represents the best-known pre-industrial period of human depopulation and rapid social change in Europe. Population growth in the 13th Century created considerable pressure on what had been largely subsistence agricultural and pastoral economies across Europe, including meeting the food demand from the growth of urban centres (Astill & Langdon 1997). The Great Famine and Black Death substantially raised mortality rates and generated major social, cultural and economic changes, though the

severity of these varied from place to place (Alfani & Murphy 2017; Benedictow 2004; Campbell 2000; Fraser 2011; Jedwab *et al.* 2022). Population levels only began to recover over the late 16th and 17th Century, a recovery paralleled by increasingly specialised agricultural systems and greater market freedoms (Hallam 1988).

Two sets of scientific literature provide opposing predictions of how floristic diversity might respond in areas that experienced 14th Century depopulation and abandonment of cultivated lands. The first hypothesis is that biodiversity levels should increase following agricultural abandonment, over approximately 10 to 75 years (with the transition from croplands and other anthromes towards intermediate-aged and mature successional vegetation) and then remain high until agriculture returns (Cramer *et al.* 2008; Hudson *et al.* 2014; Newbold *et al.* 2015). The second hypothesis predicts declines in floristic diversity in response to depopulation, farmland abandonment and the loss of anthropogenic mosaic landscapes, followed by a recovery in diversity in the following two centuries, alongside human population and cultural recovery (Armstrong *et al.* 2021; Gordon *et al.* 2024; Lomba *et al.* 2020; Niedrist *et al.* 2009; Prangel *et al.* 2023; Root-Bernstein & Svenning 2018).

We investigate these competing hypotheses using a dataset of 4,616 Common Era samples from 109 standardised European pollen records. Adopting a ‘natural experiment’ approach, we treat the abandonment of cultivated land associated with increased human mortality and socio-cultural reorganisations of the 14th Century in Europe as a test of historical human influences on biodiversity.

Materials and methods

Data processing and standardisation

We downloaded all available European pollen records from the Neotoma palaeoecology database (Williams *et al.* 2018) using the `neotoma2` R package (Vidaña & Goring 2023) and

standardised these data following the recommendations from Flantua *et al.* (2023), which we briefly outline below (see *Supporting Information: Extended Methods* for further details). We filtered the total Neotoma download based on each pollen record's (i) pollen and chronological control sampling intensity and (ii) inclusion in the Githumbi *et al.* (2022) synthesis of European Holocene vegetation change, in order to model past vegetation cover (discussed in following two sentences). For records that met these criteria, we modelled past vegetation cover for each pollen sample using the REVEALS model (Sugita 2007), with the requisite per-record input data from Githumbi *et al.* (2022). This provided proportional estimates of past vegetation cover for the dominant taxa per sample, which we multiplied by the original pollen counts [following Felde *et al.* (2016)] to help mitigate against the variation in pollen source areas, relative pollen productivity and dispersal, depositional environments, taphonomy, [etc., see Sugita (1994, 2007) and Sugita *et al.* (2010)] across the dataset, which can strongly bias pollen diversity and composition metrics (e.g., Senn *et al.* 2022). We then computed a new Bayesian age-depth model for each pollen record using **`Bchron`** (Haslett & Parnell 2008), harmonised pollen-type names using an updated harmonisation table (Birks *et al.* 2023), randomly resampled (without replacement) 150 pollen grains from each REVEALS-adjusted pollen sample using the `rrarefy` function from **`vegan`** (Oksanen *et al.* 2022) and paired each randomly resampled pollen assemblage with a random realisation ('draw') from that record's age-depth model. We then excluded all samples with assigned ages falling outside the Common Era (0 – 1850 CE). We repeated this resampling and age allocation procedure 1,000 times to generate 1,000 Common Era pollen datasets – where each sample is represented by a random age draw and resampled pollen assemblage – thereby propagating uncertainties inherent to the pollen resampling and age-depth modelling steps through our analyses.

Overall, this procedure resulted in the reduction of the initial Neotoma download down to 109 high temporal resolution European pollen records (each resampled 1,000 times), comprising

4,616 samples spanning the Common Era (see *Supporting Information: Extended Figures and Tables, Fig. 1* for sampling intensities and spatial and temporal coverage of the pollen dataset and *Supporting Information: Extended Methods* for detailed descriptions of each step summarised here).

Pollen diversity and composition metrics

We used these standardised pollen data to evaluate the consequences of the 'Black Death era' for floristic diversity by comparing the richness [the number of unique pollen types per sample (Birks & Line 1992)], evenness [how the abundances of pollen grains are distributed among pollen types (Pielou 1966)], and temporal turnover of pollen samples [the change in the abundances and types between successive samples, measured using an interval-adjusted Bray-Curtis index (Bray & Curtis 1957)], before, during and after the 14th Century. Fossil pollen data contain information on past plant compositions, though the pollen – vegetation relationship is non-linear (Davis 1963; Prentice & Webb III 1986). Despite this non-linearity, positive relationships have been identified between pollen and plant diversity across multiple regions, vegetation types and climates of Europe (e.g., Felde *et al.* 2016; Matthias *et al.* 2015; Papadopoulou *et al.* 2022; Reitalu *et al.* 2019; Senn *et al.* 2022). To estimate changes in the extent of cultivated land, we computed the REVEALS-outputted "Agricultural land" plant functional type, which represents modelled counts of pollen grains from cereal taxa (Githumbi *et al.* 2022; Wolf *et al.* 2008).

We modelled these Common Era diversity and vegetation composition datasets through time using Generalised Additive Models (GAMs), fitted with discretized predictor variables (for computational efficiency) and `bam` from **`mgcv`** (Li & Wood 2020; Wood 2011). We employed a bootstrapping and posterior simulation procedure to handle the 1,000 resampled pollen datasets (that included variation from the age-depth modelling and resampling) and to incorporate statistical uncertainty adequately in our results. We approximated the first

derivative of each simulated temporal smooth using the method of central finite differences and summarised these derivative values across draws, marking timepoints in bold where >95% of the cohort of simulations were represented by exclusively positive or negative values, and others in regular linewidth. We performed these analyses for all combinations of pollen metric, spatial unit (per-vegetation zone or European-scale) and 14th Century cereal trajectory (see below).

Comparison of landscapes with different agricultural trajectories

We compared the temporal patterns of pollen diversity and composition between landscapes with different histories of agricultural activity over the Black Death era. To do this, we decomposed the Common Era pollen diversity and composition data (Fig. 1A-D) into three categories based on the 14th Century cereal farming trajectories of individual pollen records, calculating each record's '14th Century cereal farming trajectory' as the change in average (across samples per record) cereal counts between the period 1200 – 1300 CE and the period 1400 – 1500 CE. We then modelled these categories through time using GAMs, as above. The categories were (**i**) pollen records that declined in cereal representation, thus indicating a contraction or cessation of arable farming (i.e., some degree of abandonment; Figs. 1E-H, green lines), (**ii**) pollen records where cereal cultivation continued at the same level or increased over the same period (Figs. 1E-H, orange lines), and (**iii)** pollen records that showed no evidence of cereal cultivation over the 14th Century (zero cereal grains present in samples over the 13th – 15th Centuries; Figs. 1E-H, purple lines).

Category (i), pollen catchments where cereal pollen declined over the Black Death era, could in principle include landscapes where there was a complete 'cessation' of cereal farming (i.e., records with cereal counts that declined to zero) and others where there was merely a 'decline' (i.e., records with cereal counts that declined to a non-zero value). However, we cannot distinguish such landscapes with confidence due to sample error; given the relatively low cereal counts (on average fewer than one grain per 150 grains in a rarefied resample,

Fig. 1D) and the potential for the long-distance transport of individual pollen grains. Hence, we opted for a combined 'abandonment' category, where 'abandoned' refers to any reduction in cereals, rather than necessarily the complete disappearance of cereal pollen from pollen samples.

Assessing the drivers – human-generated mosaics

Finally, we investigated how changes in vegetation structure and landscape (pollen source area) scale heterogeneity over the Black Death era related to these diversity changes (Fig. 2). European vegetative types can be (heuristically) characterised along a spectrum between fully wooded and fully open (grassland/herbaceous, including open anthromes) ecosystems. Based on expectations from the intermediate disturbance (Connell 1978; Grime 1973) and habitat heterogeneity (MacArthur 1972) hypotheses, we expect landscapes characterised by intermediate proportions of wooded and non-wooded elements to have the highest floristic diversity. If this is correct, we expect divergent trajectories of diversity change over the Black Death era depending on the 'starting condition' (wooded proportion) of each landscape's floristic assemblage. To investigate this, we firstly modelled the relationship between richness and the tree pollen percentage (which represents the coarse-level structure of Europe's vegetation: wooded and non-wooded elements) for all pollen samples that fell within the 13th Century (1200 – 1300 CE); i.e., prior to the Great Famine and Black Death. We then computed the *predicted* change in richness over the 14th Century (using the model fitted to the spatial data in Fig. 3A) that would be expected, given the (i) initial tree cover (in the 13th Century) and (ii) change in tree cover at each pollen record location across the 14th Century (i.e., between the 13th and 15th Centuries). We then plotted the *observed* change in richness over the 14th Century against these predicted changes (Fig. 3B; see Fig. 2 for a map of actual changes in each metric per pollen record over the 14th Century) to evaluate how well the modelled relationship (Fig. 3A) predicted actual richness change over the Black Death era. We performed these analyses at both whole-Europe (Fig. 3) and also vegetation

zone (Fig. 4D-I) scales, since pre-Black Death (13th Century) tree cover varied between biogeographic regions.

Results

Temporal and spatial diversity patterns of diversity change

Overall, average pollen richness and evenness increased from the start of the Common Era up to ~700 CE, followed by a period of decline and then subsequent increase from ~1000 CE up to 1300 CE (Figs. 1A & B). Following the onset of the 14th Century, average richness and evenness rapidly declined, with both metrics falling to the approximate level they had been 1,000 years earlier. After ~150 years of steep decline, both richness and evenness increased again, returning to their late 13th Century peak by ~1650 CE (Figs. 1A & B) and increasing to the final time point considered here (1850 CE). Floristic turnover remained relatively stable, or slightly reduced, over the first ~500 years of the Common Era but accelerated after ~600 CE up to the 1850 CE (Fig. 1C).

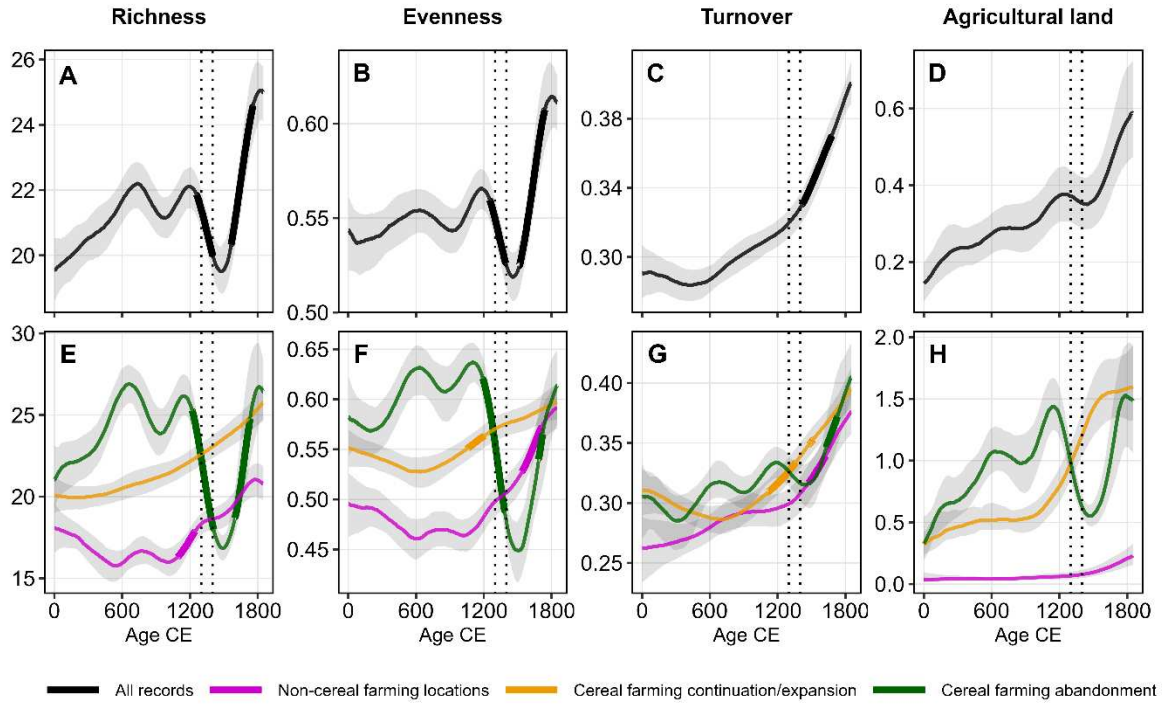

Fig. 1. Common Era diversity metrics. Generalised additive models fit to **(A, E)** richness (number of unique pollen types), **(B, F)** evenness (Pielou Index), **(C, G)** turnover (Bray-Curtis dissimilarity through time) and **(D, H)** Agricultural land (REVEALS-modelled cereal counts per 150 grains) as a smooth function of time. Panels **A-D** show results across all pollen records (black); panels **E-H** show results split into areas where cereal farming declined (green, n = 32) or remained stable/increased (orange, n = 62) over the 14th Century, with non-cereal farming locations shown in purple (n = 15). Central lines represent the average fit across the 1,000 resamples, with sections of thicker lines indicating periods over which >95% of the smooths exhibit positive or negative slopes. Slope percentiles are not shown for Agricultural land because the direction of change is predetermined by the subsetting of records by cereal trajectory. Grey intervals represent interquartile range across fits to each of the 1,000 resamples. Vertical black dotted lines show the bounds of the 14th Century. Sample sizes per coloured line in **(E-H)** are computed by calculating the mean change in cereals over the 14th Century across the 1,000 resamples, then identifying the category of change. Note though that individual resamples (of the 1,000) per pollen record may not all show the same cereal trajectory (given the random variation in pollen assemblage compositions across the 1,000 arising from our resampling procedure). Total pollen record N = 109.

Agricultural land, estimated from cereal counts, also increased overall from 0 CE up to ~1250 - 1300 CE, with a fluctuation between ~700 and 1000 CE. Agricultural land extent then declined to ~1450 CE and gradually increased thereafter up to 1850 CE (Fig. 1D). Hence, richness and evenness changes follow those of agricultural cereal trends (*Supporting Information: Extended Figures and Tables, Extended Fig. 2*). These two diversity metrics remained lower than the pre-1300 CE levels for ~300 years, a duration mirroring that of human population and of societal and agricultural recovery in Europe after the crises of the 14th Century.

Despite these clear average temporal patterns (Fig. 1), trajectories of change at individual sites over the Black Death era (Fig. 2; calculated as the change per site in each average metric between 1200 – 1300 CE and 1400 – 1500 CE) were spatially heterogeneous. For richness, evenness and turnover, there were some sites that increased and others that decreased over the full range of European latitudes and longitudes (Fig. 2A-C). Change in the extent of agricultural land (Fig. 2D) and tree cover change (Fig. 2E) were also spatially heterogeneous. Different directions of per-site changes in each metric were observed within each broad vegetation type (Fig. 2), suggesting landscape-scale responses, but there were nonetheless different average biodiversity responses that reflected differences in average levels of pre-Black Death forest cover in each vegetation region (see below, Fig. 4).

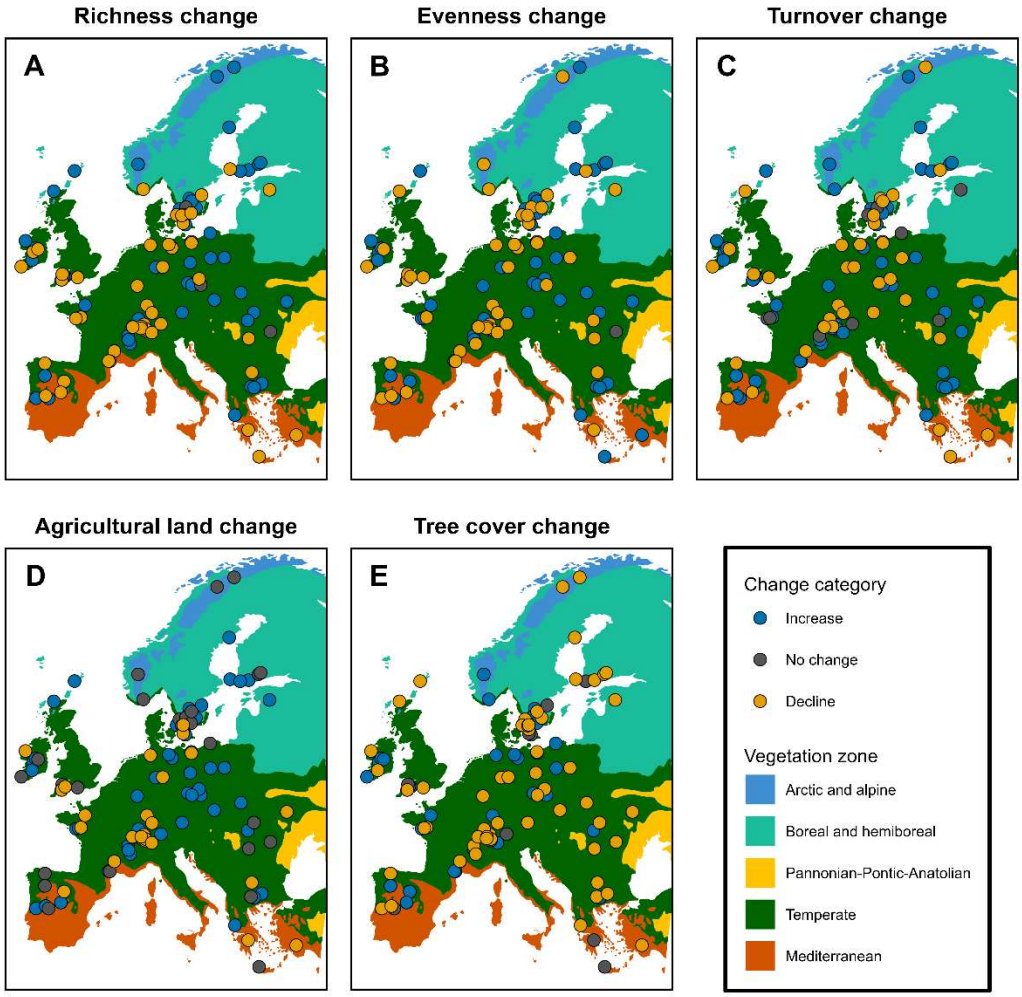

Fig. 2. Change in diversity metrics, turnover and agricultural land area over the Black Death era (spanning the 14th Century). Points represent the change in **(A)** richness, **(B)** evenness, **(C)** turnover, **(D)** agricultural land (REVEALS-modelled cereal counts) and **(E)** tree cover (percentage) at individual pollen sites between two time windows: Time window 1 = 1200 – 1300 CE and time window 2 = 1300 – 1400 CE (averages of samples per site, for the two centuries; see *Methods*). Yellow points represent declines in each metric, blue points represent increases and grey points represent no change (plus or minus five percent). Coloured polygons represent Europe's primary vegetation zones from Lang *et al.* (2023). Total pollen record N = 109.

The overall downturn in European cereal pollen was relatively modest (Fig. 1D) because the effects of the Great Famine and Black Death were not spatially uniform across Europe, with the extent and nature of agricultural practices and its impacts varying both within and between regions (Fig. 2). Temporal diversity patterns from pollen records that either remained unchanged or increased in cereal representation over the 14th Century show diversity gains from the 7th Century up to 1850 CE (Figs. 1E-G, orange lines). However, those landscapes that experienced declines in cereal cultivation strongly declined in richness and evenness from ~1300 CE, reaching minima ~1450 CE, but increasing thereafter (Figs. 1E-F, green lines). Average richness and evenness values were substantially lower for non-cereal farming locations than for the other two categories over the period 0 – 1300 CE (Figs. 1E-F, purple lines), with richness and evenness values at abandoned sites declining to less than or approximately the same values as those non-cereal farming sites over the Black Death era (compare Figs. 1E-F green and purple lines). Differences between the three categories in the magnitude of turnover changes were much smaller (Fig. 1G). Plotting cereals by these same categories (Fig. 1H) shows the similarity of temporal trends for cereal pollen, richness and evenness for those sets of pollen records that reveal declines in cereal farming activity across the 14th Century.

Together, these data show that the diversity declines observable in the full diversity datasets (Figs. 1A-C) were driven by declining diversity metrics in landscapes where cereal cultivation had been at relatively high levels up to ~1300, but where cereal cultivation declined or was abandoned in the 14th Century (Figs. 1E-G). It is worth noting that pollen counts from cereals represent a very small proportion of the total count (between zero and two grains per 150 on average, Fig. 1D), so cereal cultivation did not dominate Europe's landscapes over the period considered here - they indicate the presence of human cereal farming and, by implication, other human activities (such as rearing livestock, erecting buildings, establishing boundaries, paths and tracks, and managing woodlands) within multi-use landscapes.

Changes in landscape heterogeneity

Our analyses reveal a 'hump-shaped' relationship between richness and tree cover, with expected average richness maximised at approximately 40% tree cover (Fig. 3A; and also maximised for intermediate levels of cereal pollen, *Supporting Information: Extended Figures and Tables, Extended Fig. 3*). This is consistent with the heterogeneity hypothesis (MacArthur 1972), whereby very open (here, <30% tree cover) landscapes are expected to increase in diversity with the expansion of tree cover, while tree cover expansion beyond ~50% is expected to erode diversity. Plotting the observed change in richness over the 14th Century against changes predicted from the change in tree cover over the same period (see Fig. 2 for a map of actual changes in each metric per pollen record over the 14th Century) reveals a positive relationship between the model-predicted and observed richness change values, verifying that the model (in Fig. 3A) is capturing the general trend in changes to richness predicted by changes in tree cover across the 14th Century (Fig. 3B). This shows that landscapes with vegetation that moved towards intermediate tree cover over the Black Death era resulted in richness gains, whereas those landscapes that moved towards the extremes resulted in richness losses. Given that humans were major drivers of changes to European woodland extent from the Neolithic onwards (Roberts *et al.* 2018), these results support our overall interpretation that landscapes with intermediate levels of human landscape-scale modification represent higher diversity floristic communities.

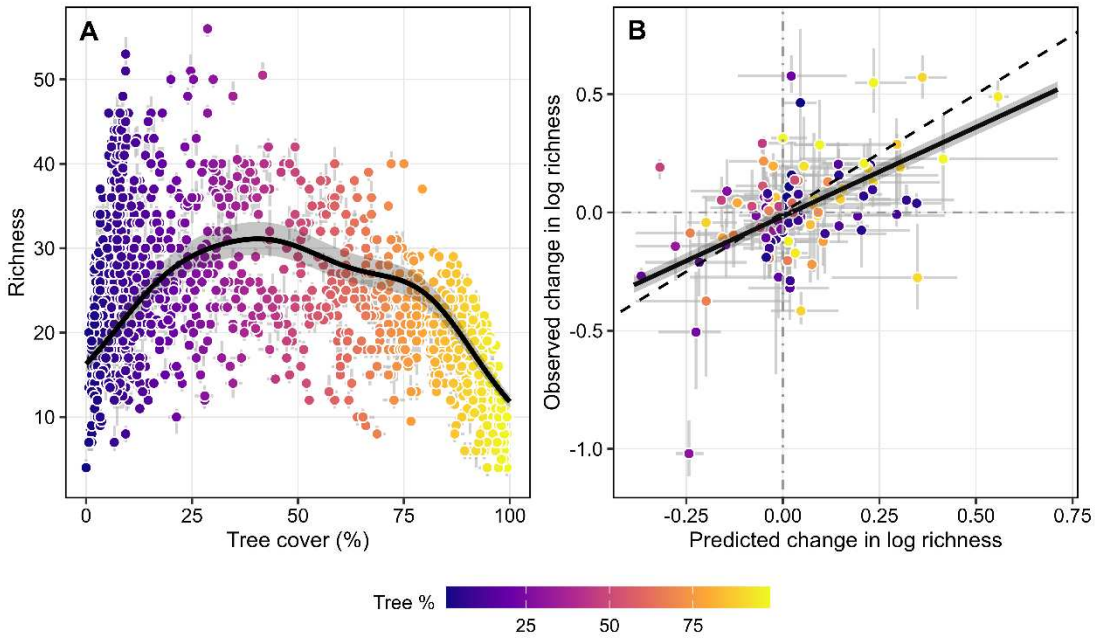

Fig. 3. Tree representation and richness relationships. (A) Richness as a nonlinear function of percentage tree cover (1200 – 1300 CE), see *Supporting Information: Extended Figures and Tables, Extended Table 1* for model summary (N unique pollen samples = 1,449). **(B)** Predicted versus observed change in log richness across the 14th Century, see *Supporting Information: Extended Figures and Tables, Extended Table 1* for model summary (N pollen records = 109). The values along the x-axis in panel **B** are computed by calculating the expected richness change given the change in tree cover estimated from the fitted non-linear function shown in panel **A**. For example, if a pollen record increased in tree cover from an initial 5% in the period 1200 – 1300 CE to 10% tree cover in the period 1400 – 1500 CE, there would be an expected richness change of +5. The values along the y-axis in panel **B** are computed by calculating the difference in richness (from the empirical pollen data) between the period 1200 – 1300 CE and 1400 – 1500 CE. In both panels, the central points represent the median and the crosshairs represent the variation (25th and 75th percentiles) across the 1,000 resamples in both (change in) richness and percentage tree cover. Points are coloured by their tree percent in the 13th Century (shown on the x-axis in panel **A**). Model summaries are presented in *Supporting Information, Appendix 1.*

Different vegetation zones exhibited different average trajectories of Common Era temporal richness patterns (Figs. 4A-C), but the underlying processes appear to be the same: (i) locations characterised by intermediate tree cover were associated with maximum richness (Fig. 4D-F) and (ii) change in richness predicted per landscape from the change in tree cover between the periods 1200 – 1300 CE and 1400 – 1500 CE was strongly related to observed changes in richness at individual sites (Fig. 4G-I).

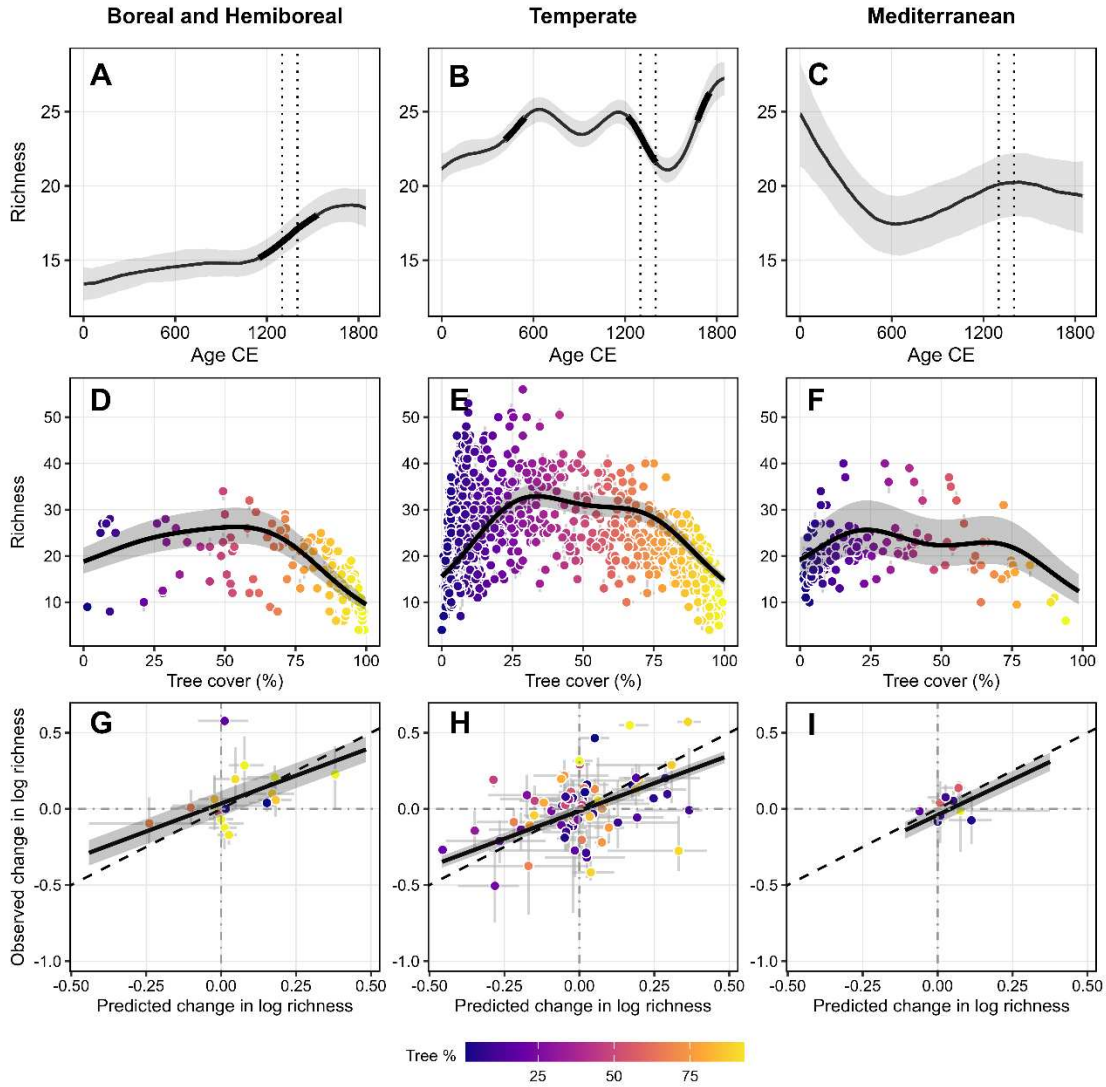

Fig. 4. Per-vegetation zone (A-C) temporal richness patterns and (D-I) tree representation and richness relationships. (A-C) Generalised additive models fit to richness as a smooth function of time. Central lines represent the average fit across the

fitted distribution (see *Methods*), with sections of thicker lines indicating periods over which >95% of the draws exhibit positive or negative slopes. Grey intervals represent the interquartile range across draws. Vertical black dotted lines show the 14th Century. **(D-F)** Richness as a nonlinear function of percentage tree cover (1200 – 1300 CE) for each vegetation zone, see *Supporting Information: Extended Figures and Tables, Extended Table 2* for model summaries. **(G-I)** Predicted change in log richness versus observed change in log richness across the 14th Century; see *Supporting Information: Extended Figures and Tables, Extended Table 3* for model summaries. In all panels, the central points represent the median and the crosshairs represent the variation (25th and 75th percentiles) across the 1,000 resamples. Points in panels **D-I** are coloured by their tree percent in the 13th Century (shown on the x-axes in panels **D-F).**

Discussion

Using 14th Century famine and disease in Europe as a test case, we find that abandonment or decreases in arable farming (with associated farming and rural management activities) led to declines in biodiversity metrics over the following one to two centuries. For those pollen records with evidence of cereal decline (Fig. 1H, green line; Fig 2D, yellow points), we identify three phases of diversity change over the Common Era (up to 1850 CE), which we suggest are directly linked to changing human landscape management practices (at the scale of relevant pollen source areas, ~landscapes) and their impacts on the heterogeneity of habitats per unit area within a landscape (Fig. 5).

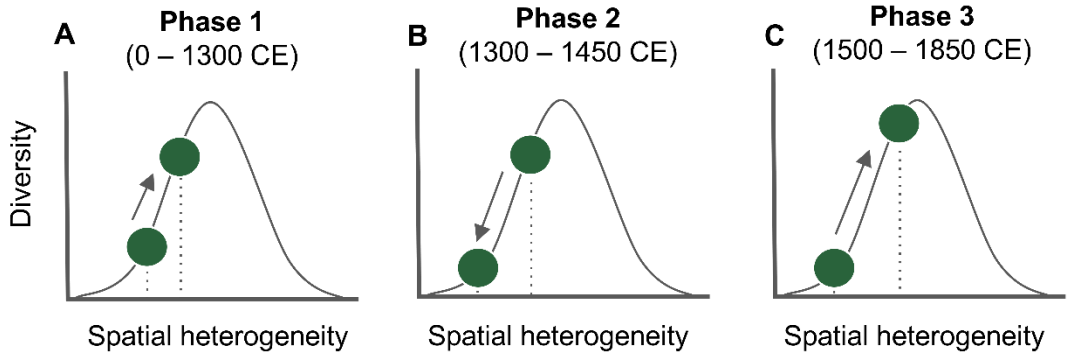

Fig. 5. Schematic representation of changes to floristic diversity across the Common Era in European landscapes that experienced cereal abandonment during the 14th century. Green circles represent the average diversity changes in relation to changes in spatial heterogeneity of pollen source areas surrounding European pollen records (~landscapes), for three time periods. See main text for additional interpretation.

Phase one (0 – 1300 CE) represents an expansion of arable practices (Fig. 1D & H) as human populations grew, changing those landscapes in ways that generated mosaics of different habitats and increasingly diverse floristic assemblages (Fig. 1, Fig. 5A). The period 0 – 900 CE includes the expansion, maximum extent and later the retreat (during the 5th century) of the Western Roman empire from southern Europe and beyond. Roman agricultural systems were highly market oriented and their expansion over the period 0 – 400 CE (Fig. 1D & H) was driven by an increasing nutritional demand from the Empire's growing urban populations (administrators, crafts people, etc.) and its substantial military (Allen & Lodwick 2017). The increased tax burden from the Roman administration necessitated the expansion of provincial grain production, with an expanded road network and investment in grain drying and storage facilities facilitating its long-distance transport (Van der Veen 2016). In the Mediterranean zone, production focussed on olives and grapes, with cereal and other crops frequently grown in a diverse matrix. Outside of the Roman frontiers (i.e., much of northern central and north eastern Europe), populations relied heavily upon barley and later rye, often cultivated in mixed systems with a strong emphasis on raising cattle (Behre 1992;

Grabowski 2013; Lange 1975). Despite these regional differences, European arable production increased over the first 400 years of the Common Era, a trend that continued into the Early Middle Ages (from 500 CE onwards; Fig. 1). In England, for example, the post Roman period saw little woodland regeneration and settled areas remained open (Rippon *et al.* 2015). However, in some areas there were significant changes when agriculture shifted from small-scale relatively intensive regimes to extensive, low-input, larger-scale regimes by 800 – 900 CE (Hamerow 2022). The period 680 – 830 CE saw several new features appearing in Europe's landscape such as ditched enclosures to corral livestock and centralised crop processing and storage, suggesting more extensive arable cultivation and grain surpluses, yet still within a very mixed agrarian landscape (Hamerow 2022).

Our data therefore do not support a 'collapse' of provincial rural agriculture after Roman withdrawal in the 5th Century (Faulkner 2000; McCormick 2002; Ward-Perkins 2005), instead it supports the view of a restructuring of post-Roman markets, economies and elites (Wickham 2009) in unison with continued arable production. Thus, diversity measures continued to increase in association with expanding arable production over the Early Middle Ages, up to ~700 CE (Fig. 1A & E).

The period 700 – 900 CE had roughly stable (perhaps slightly reducing) arable production and moderately reducing diversity values. Yet, from ~900 CE onwards, European populations grew and the total area under cultivation expanded once again, particularly in the more densely populated areas of north-western Europe (Duby 1962; Hoffmann 2014; Mitterauer 2010). Enabled by innovations such as the heavy mouldboard plough, the use of horses as draught animals, and three-year crop rotations with extensive use of fallowing, arable cultivation was extended onto previously unploughed woodland, wastelands, pastures and wetlands. New crops such as oats and rye were also introduced to exploit poor soils, particularly in upland regions (Litt *et al.* 2009). Open fields with intermingled strips and some degree of collective management are documented in many regions from 1000 CE onwards,

such as in the midlands of England (Leturcq 2007; Schroeder 2022; Thoen 2018). Elsewhere, for example across Scandinavia, a single ‘infield’ of small plots of fields were surrounded by large open areas of meadows, and pastures at some distance from the infield, that could be brought into temporary arable cultivation when needed, or that could be intermingled with other enclosed land, forming a patchwork of cropping regimes (Nesset & Hjelle 2022; Thoen 2018).

During Phase one, Europe’s expanding and diverse mosaics of cultivated lands were typically separated by woods, heath, or uncultivated plots, and often enclosed by hedgerows or trees (Verhulst 2002). Europe’s agro-ecosystems thus represented a complex lattice of multiple agricultural practices operating within remnants of ‘natural’ (e.g., forests, bogs) and ‘semi-natural’ (e.g., grasslands, heathlands) areas in many European regions, and diversity metrics were correspondingly high (Figs. 1 & 4). In addition to the different elements of the mosaic, edge effects and ecotones would have contributed to the overall raised floristic diversity at this time.

Phase two (1300 – 1450 CE) represents a sharp decline in diversity during and immediately following the Black Death era (Fig. 5B), with the strongest impacts within the temperate zone, particularly north western Europe (Fig. 2). During this period, the decline in human populations and resulting social and cultural reorganization led to the reduction or cessation of arable farming in many regions across Europe (Dodds 2008). Relatively recent settlements that had been established in more marginal locations as the population grew, and which required greater labour and resource inputs to sustain, were more vulnerable to abandonment (Green & Mair 2025), whereas larger more established settlements with preferential trade routes or resources might have experienced consolidation or population growth, as surviving communities migrated. The reduction or full withdrawal of cultivation reduced spatial heterogeneity within many landscapes across Europe, thereby driving floristic diversity declines in these areas (Figs. 1 & 2D).

However, biodiversity responses to Black Death land-use changes varied significantly by location (Fig. 2) (Yeloff & Van Geel 2007) due to differences in the 'starting condition' of vegetation compositions (i.e., amount of tree cover) in the century before the Black Death. Our analysis – based on records from across multiple vegetation zones and latitudes – reveals a non-linear relationship where diversity peaked at intermediate levels of tree cover (~40%, Figs. 3 & 4D-I). Consequently, diversity declined in landscapes that shifted towards extremes (either heavily wooded or very open) but increased in those landscapes that shifted towards intermediate tree cover states over the 14th century. Thus, reduction or cessation of arable production did not universally reduce biodiversity. In previously very open landscapes (<30% tree cover), woodland regeneration increased habitat heterogeneity and drove richness gains (e.g., records in Northern Germany, Northern France, Western Spain; increasing richness and tree cover, blue points in Figs. 2A & E). Conversely, in regions with higher initial tree cover (>50%), diversity changes were positively linked to openness. A recent study based on six pollen records from southern Germany finds that reduced arable production was associated with floristic diversity declines over this period (decreasing cereals, yellow points; Fig. 2D) (Spitzig *et al.* 2025), whilst in other areas such as Bohemia, agricultural expansion over the 14th Century and the transition from a forest-based economy to an agricultural one (Myśliwski 2011) resulted in diversity gains (increasing cereals, blue points; Fig. 2D). Our whole-continent analyses reveal that Black Death era diversity responses were determined by whether land-use changes moved a landscape closer to, or further from, an optimal intermediate state of tree cover, rather than by a linear relationship with openness.

Finally, Phase three (1450 – 1850 CE) represents a gradual agrarian recovery in the aftermath of the Black Death as economies across Europe regenerated, and population levels gradually responded. Increasing market engagement, including long distance trade, resulted in a specialised and diverse emerging European agricultural economy from the 16th Century e.g. (Overton 1996), the result of which was to drive diversity back up, increasing up

to the end of the study period (1850 CE; Fig. 5D). Meanwhile, the changing practices and pressures of the period led to continuing growth of arable land in other landscapes (i.e., increased cereal pollen frequencies) from before 1100 CE through to ~1500 CE, and with it increased richness, evenness and community turnover (orange lines in Figs. 1E-H). For example, the well-established and persistent mixed farming practices associated with subsistence farming in Central Europe and parts of southern Scandinavia. In non-arable landscapes (i.e., those with zero cereal pollen in samples 1200 – 1500 CE), richness, evenness and turnover also increased, especially after 1500 CE, most likely associated with increased pastoral farming and woodland management in 'marginal' landscapes (purple lines in Figs. 1E-H).

Overall, these results support our hypothesis that increases in human population densities and accelerating farming-associated landscape modification increased Europe's floristic diversity from the early-mid Holocene onwards, up to the final date considered here, 1850 CE (Gordon *et al.* 2024), a trend that was temporarily reversed in some areas by depopulation, land abandonment and the economic and social shifts that followed the Great Famine and Black Death. Diversity declines were associated with locations where cereal representation was reduced or disappeared over the 14th Century (Fig. 1D-H). However, the precise course of events depended on the prior environmental conditions of the landscapes under consideration, i.e., the starting woodland cover (Figs. 3 & 4D-I). The different 'starting states' may also help explain discrepancies between the conclusions of biodiversity responses in the palaeoecological versus more recent record (e.g. these results cf. Newbold *et al*., 2015). Over the full period considered here – and the three types of landscapes that were characterised by different arable farming histories – richness and evenness tracked agriculture and, through it, human development, culture, and population growth, collapse, and recovery. This reveals positive effects of traditional rural activities and human-created mosaics of habitats on biological diversity. In turn, these human-generated (novel), diverse

systems supported novel and varied assemblages of other groups of taxa, such as farmland birds (Carroll et al. 2023).

Remnants of these diverse, human-generated landscapes can still be found, with traditionally-managed locations and regions that escaped intensification in the late 18th to 20th Century representing many of the most biodiverse present-day landscapes across Europe (regions categorised as 'High Nature Value' farmlands by the European Environment Agency (EEA 2004). These landscapes typically represent agro-ecological systems characterised by low intensity grazing and mixed farming methods, and include *inter alia* the Iberian *dehesas* and *montados* (low intensity agro-forestry systems), Alpine pastures, Baltic wood pastures, the Hungarian *Tanya* (small-scale mixed farming systems) and the Nordic Alvar pastures (semi-natural grasslands) (Lomba *et al.* 2020). Thus, the legacies of the low intensity, mixed farming systems of Europe's Middle Ages remain present today across the continent. These landscapes have dual cultural and biodiversity value but are today considered at risk of abandonment, with associated loss of heterogeneity and biodiversity. For example, land abandonment and loss of extensive grazing systems has led to encroachment of shrubs and increasing risk of wildfires (Feurdean et al. 2017; Shakesby 2011), both of which may erode aspects of biodiversity. This is increasingly recognised by governments and others who offer subsidies to farmers to support the persistence of traditional, or equivalent, management practices such as the reintroduction of extensive grazing to restore heterogeneity and biodiversity, and to reduce fire risks (Rouet-Leduc *et al.* 2021; Streifeneder *et al.* 2022).

In summary, we used the abandonment of cultivated land associated with increased human mortality and socio-cultural reorganisations of the 14th Century in Europe as a test of historical human influences on biodiversity. Our work suggests that human-associated activities underpinned the major European floristic diversity gains that occurred over the last 12,000 years, the legacies of which are highly valued today across the continent as

biodiversity hotspots and culturally-valued landscapes. These findings underline the interconnections of people and biodiversity and support the reinstatement of certain types of 'traditional' agriculture to support biodiversity, an approach that might be particularly suitable in regions where other measures, such as strict protection and landscape-scale disturbance using large animals ('rewilding'), are not feasible or desirable.

References

Abraham, V., Oušková, V. & Kuneš, P. (2014). Present-Day Vegetation Helps Quantifying Past Land Cover in Selected Regions of the Czech Republic. *PLOS ONE*, 9, e100117.

Alfani, G. & Murphy, T.E. (2017). Plague and Lethal Epidemics in the Pre-Industrial World. *J. Econ. Hist.*, 77, 314–343.

Allen, M. & Lodwick, L. (2017). Agricultural Strategies in Roman Britain. In: *The Rural Economy of Roman Britain. New Visions of the Countryside of Roman Britain*. Society for the Promotion of Roman Studies, pp. 142–177.

Armstrong, C.G., Miller, J.E.D., McAlvay, A.C., Ritchie, P.M. & Lepofsky, D. (2021). Historical Indigenous Land-Use Explains Plant Functional Trait Diversity. *Ecol. Soc.*, 26, art6.

Astill, G. & Langdon, J. (1997). *Medieval Farming and Technology: The Impact of Agricultural Change in Northwest Europe*. Brill.

Behre, K.-E. (1992). The history of rye cultivation in Europe. *Veget Hist Archaeobot*, 14, 141–156.

Benedictow, O.J. (2004). *The Complete History of the Black Death*. Boydell & Brewer, Woodbridge, UK.

Birks, H.J.B., Bhatta, K.P., Felde, V.A., Flantua, S.G.A., Mottl, O., Haberle, S.G., *et al.* (2023). Approaches to pollen taxonomic harmonisation in Quaternary palynology. *Rev. Palaeobot. Palynol.*, 319, 104989.

Birks, H.J.B. & Line, J.M. (1992). The use of Rarefaction Analysis for Estimating Palynological Richness from Quaternary Pollen-Analytical Data. *The Holocene*, 2, 1–10.

Bray, J.R. & Curtis, J.T. (1957). An Ordination of the Upland Forest Communities of Southern Wisconsin. *Ecol. Monogr.*, 27, 325–349.

Campbell, B.M.S. (2000). *English Seigniorial Agriculture 1250-1450*. Cambridge University Press, Cambridge, UK.

Carroll, T., Hatfield, J.H. & Thomas, C.D. (2023). Globally abundant birds disproportionately inhabit anthropogenic environments.

Connell, J.H. (1978). Diversity in Tropical Rain Forests and Coral Reefs. *Science*, 199, 1302–1310.

Cramer, V.A., Hobbs, R.J. & Standish, R.J. (2008). What's new about old fields? Land abandonment and ecosystem assembly. *Trends Ecol. Evol.*, 23, 104–112.

Davis, M.B. (1963). On the theory of pollen analysis. *Am. J. Sci.*, 261, 897–912.

Dodds, B. (2008). Patterns of Decline: Arable Production in England, France and Castile, 1370–1450. In: *Agriculture and Rural Society after the Black Death: Common Themes and Regional Variations* (eds. Dodds, B. & Britnell, R.H.). University of Hertfordshire Press, pp. 164–186.

Duby, G. (1962). *L'économie rurale et la vie des campagnes dans l'Occident médiéval (France, Angleterre, Empire, IXe–XVe siècles): Essai de synthèse et perspectives de recherches*. Aubier, Paris.

EEA. (2004). *High nature value farmland - Characteristics, trends and policy challenges* (Publication). European Environment Agency, Copenhagen.

Faulkner, N. (2000). *The Decline and Fall of Roman Britain*. Tempus, Stroud.

Felde, V.A., Peglar, S.M., Bjune, A.E., Grytnes, J.-A. & Birks, H.J.B. (2016). Modern pollen–plant richness and diversity relationships exist along a vegetational gradient in southern Norway. *The Holocene*, 26, 163–175.

Feurdean, A., Munteanu, C., Kuemmerle, T., Nielsen, A.B., Hutchinson, S.M., Ruprecht, E., *et al.* (2017). Long-term land-cover/use change in a traditional farming landscape in Romania inferred from pollen data, historical maps and satellite images. *Reg. Environ. Change*, 17, 2193–2207.

Flantua, S.G.A., Mottl, O., Felde, V.A., Bhatta, K.P., Birks, H.H., Grytnes, J.-A., *et al.* (2023). A guide to the processing and standardization of global palaeoecological data for large-scale syntheses using fossil pollen. *Glob. Ecol. Biogeogr.*, 32, 1377–1394.

Fraser, E.D.G. (2011). Can economic, land use and climatic stresses lead to famine, disease, warfare and death? Using Europe's calamitous 14th century as a parable for the modern age. *Ecol. Econ.*, Special Section: Ecological Economics and Environmental History, 70, 1269–1279.

Fyfe, R.M., de Beaulieu, J.-L., Binney, H., Bradshaw, R.H.W., Brewer, S., Le Flao, A., *et al.* (2009). The European Pollen Database: past efforts and current activities. *Veg. Hist. Archaeobotany*, 18, 417–424.

Giesecke, T., Ammann, B. & Brande, A. (2014). Palynological richness and evenness: Insights from the taxa accumulation curve. *Veg. Hist. Archaeobotany*, 23, 217–228.

Githumbi, E., Fyfe, R., Gaillard, M.-J., Trondman, A.-K., Mazier, F., Nielsen, A.-B., *et al.* (2022). European pollen-based REVEALS land-cover reconstructions for the Holocene: methodology, mapping and potentials. *Earth Syst. Sci. Data*, 14, 1581–1619.

Gordon, J.D., Fagan, B., Milner, N. & Thomas, C.D. (2024). Floristic diversity and its relationships with human land use varied regionally during the Holocene. *Nat. Ecol. Evol.*, 8, 1459–1471.

Goring, S., Lacourse, T., Pellatt, M.G. & Mathewes, R.W. (2013). Pollen assemblage richness does not reflect regional plant species richness: a cautionary tale. *J. Ecol.*, 101, 1137–1145.

Grabowski, R. (2013). Cereal cultivation in east-central Jutland during the Iron Age, 500 BC–AD 1100. *Dan. J. Archaeol.*, 2, 164–196.

Green, A.S. & Mair, S. (2025). Material Flow Analysis for Archaeology: A Preliminary Account of Medieval Social Metabolism Using the Excavation Archive from Wharram Percy. *J. Archaeol. Sci.*

Grime, J.P. (1973). Competitive Exclusion in Herbaceous Vegetation. *Nature*, 242, 344–347.

Hallam, H.E. (1988). Population movements in England, 1086-1350. In: *The agrarian history of England and Wales* (ed. Hallam, H.E.). Cambridge, pp. 508–93.

Hamerow, H. (2022). The “FeedSax” Project: Rural Settlements and Farming in Early Medieval England. In: *New Perspectives on the Medieval Agricultural Revolution: Crop, Stock and Furrow* (eds. McKerracher, M. & Hamerow, H.). pp. 3–24.

Haslett, J. & Parnell, A. (2008). A simple monotone process with application to radiocarbon-dated depth chronologies. *J. R. Stat. Soc. Ser. C Appl. Stat.*, 57, 399–418.

Hoffmann, R. (2014). *An Environmental History of Medieval Europe*. Cambridge University Press, Cambridge.

Hudson, L.N., Newbold, T., Contu, S., Hill, S.L.L., Lysenko, I., De Palma, A., *et al.* (2014). The PREDICTS database: a global database of how local terrestrial biodiversity responds to human impacts. *Ecol. Evol.*, 4, 4701–4735.

IPBES. (2019). *Global assessment report on biodiversity and ecosystem services of the Intergovernmental Science-Policy Platform on Biodiversity and Ecosystem Services*. IPBES Secretariat, Bonn, Germany.

Izdebski, A., Guzowski, P., Poniat, R., Masci, L., Palli, J., Vignola, C., *et al.* (2022). Palaeoecological data indicates land-use changes across Europe linked to spatial heterogeneity in mortality during the Black Death pandemic. *Nat. Ecol. Evol.*, 6, 297–306.

Jedwab, R., Johnson, N.D. & Koyama, M. (2022). The Economic Impact of the Black Death. *J. Econ. Lit.*, 60, 132–178.

Krausmann, F., Erb, K.-H., Gingrich, S., Haberl, H., Bondeau, A., Gaube, V., *et al.* (2013). Global human appropriation of net primary production doubled in the 20th century. *Proc. Natl. Acad. Sci.*, 110, 10324–10329.

Lang, G., Tinner, W., Morales-Molino, C., Schwörer, C. & Ammann, B. (2023). Late-glacial and Holocene vegetation changes and their causes. In: *Quaternary vegetation dynamics of Europe* (eds. Lang, G., Ammann, B., Behre, K.-E. & Tinner, W.). Haupt Verlag, Bern.

Lange, D.E. (1975). The development of agriculture during the first millennium A.D. *Geol. Fören. Stockh. Förh.*

Leturcq, S. (2007). *Un village, la terre et ses hommes: Toury en Beauce, XIIe–XVIIesiècle*. Éditions du CTHS, Paris.

Li, Z. & Wood, S.N. (2020). Faster model matrix crossproducts for large generalized linear models with discretized covariates. *Stat. Comput.*, 30, 19–25.

Litt, T., Schölzel, C., Kühl, N. & Brauer, A. (2009). Vegetation and Climate History in the Westeifel Volcanic Field (Germany) during the Past 11,000 Years Based on Annually Laminated Lacustrine Maar Sediments. *Boreas*, 38, 679–690.

Lomba, A., Moreira, F., Klimek, S., Jongman, R.H., Sullivan, C., Moran, J., *et al.* (2020). Back to the future: rethinking socioecological systems underlying high nature value farmlands. *Front. Ecol. Environ.*, 18, 36–42.

MacArthur, R.H. (1972). *Geographical Ecology: Patterns in the Distribution of Species*. Harper & Row, New York.

Matthias, I., Semmler, M.S.S. & Giesecke, T. (2015). Pollen diversity captures landscape structure and diversity. *J. Ecol.*, 103, 880–890.

McCormick, M. (2002). *The Origins of the European Economy: Communications and Commerce AD 300–900*. Cambridge University Press, Cambridge.

Meltsov, V., Poska, A., Odgaard, B.V., Sammul, M. & Kull, T. (2011). Palynological richness and pollen sample evenness in relation to local floristic diversity in southern Estonia. *Rev. Palaeobot. Palynol.*, 166, 344–351.

Mitterauer, M. (2010). *Why Europe? The Medieval Origins of Its Special Path*. University of Chicago Press, Chicago.

Nesset, T. & Hjelle, K.L. (2022). Settlement and Subsistence Strategies in Western Norway: Examples from Two Deserted Medieval Farms. In: *Expanding Horizons: Settlement Patterns and Outfield Land Use in the Norse North Atlantic*, University of Bergen Archaeological Series (eds. Mooney, D.E., Guðmundsdóttir, L., Dahl, B., Roberts, H. & Ramstad, M.). pp. 129–151.

Newbold, T., Hudson, L.N., Hill, S.L.L., Contu, S., Lysenko, I., Senior, R.A., *et al.* (2015). Global effects of land use on local terrestrial biodiversity. *Nature*, 520, 45–50.

Niedrist, G., Tasser, E., Lüth, C., Dalla Via, J. & Tappeiner, U. (2009). Plant diversity declines with recent land use changes in European Alps. *Plant Ecol.*, 202, 195–210.

Oksanen, J., Simpson, G.L., Blanchet, F.G., Kindt, R., Legendre, P., Minchin, P.R., *et al.* (2022). *_vegan: Community Ecology Package_. R package version 2.6-2, \textlesshttps://CRAN.R-project.org/package=vegan\textgreater.*

Overton, M. (1996). *Agricultural Revolution in England: The Transformation of the Agrarian Economy, 1500–1850*. Cambridge University Press, Cambridge.

Papadopoulou, M., Tsiripidis, I., Panajiotidis, S., Fotiadis, G., Veres, D., Magyari, E., *et al.* (2022). Testing the potential of pollen assemblages to capture composition, diversity and ecological gradients of surrounding vegetation in two biogeographical regions of southeastern Europe. *Veg. Hist. Archaeobotany*, 31, 1–15.

Pedersen, E.J., Miller, D.L., Simpson, G.L. & Ross, N. (2019). Hierarchical generalized additive models in ecology: An introduction with mgcv. *PeerJ*, 2019, e6876–e6876.

Pielou, E.C. (1966). The measurement of diversity in different types of biological collections. *J. Theor. Biol.*, 13, 131–144.

Prangel, E., Kasari-Toussaint, L., Neuenkamp, L., Noreika, N., Karise, R., Marja, R., *et al.* (2023). Afforestation and abandonment of semi-natural grasslands lead to biodiversity loss and a decline in ecosystem services and functions. *J. Appl. Ecol.*, 60, 825–836.

Prentice, I.C. (1985). Pollen representation, source area, and basin size: Toward a unified theory of pollen analysis. *Quat. Res.*, 23, 76–86.

Prentice, I.C. & Webb III, T. (1986). Pollen percentages, tree abundances and the Fagerlind effect. *J. Quat. Sci.*, 1, 35–43.

R Core Team. (2022). *R: A Language and Environment for Statistical Computing*. R Foundation for Statistical Computing, Vienna, Austria.

Reimer, P.J., Austin, W.E.N., Bard, E., Bayliss, A., Blackwell, P.G., Ramsey, C.B., *et al.* (2020). The IntCal20 Northern Hemisphere Radiocarbon Age Calibration Curve (0–55 cal kBP). *Radiocarbon*, 62, 725–757.

Reitalu, T., Bjune, A.E., Blaus, A., Giesecke, T., Helm, A., Matthias, I., *et al.* (2019). Patterns of modern pollen and plant richness across northern Europe. *J. Ecol.*, 107, 1662–1677.

Rippon, S., Smart, C. & Pears, B. (2015). *The Fields of Britannia: Continuity and Change in the Late Roman and Early Medieval Landscape*. Oxford University Press, Oxford.

Roberts, N., Fyfe, R.M., Woodbridge, J., Gaillard, M.-J., Davis, B. a. S., Kaplan, J.O., *et al.* (2018). Europe's lost forests: a pollen-based synthesis for the last 11,000 years. *Sci. Rep.*, 8, 716.

Root-Bernstein, M. & Svenning, J.-C. (2018). Human paths have positive impacts on plant richness and diversity: A meta-analysis. *Ecol. Evol.*, 8, 11111–11121.

Rouet-Leduc, J., Pe'er, G., Moreira, F., Bonn, A., Helmer, W., Shahsavan Zadeh, S.A.A., *et al.* (2021). Effects of large herbivores on fire regimes and wildfire mitigation. *J. Appl. Ecol.*, 58, 2690–2702.

Schroeder, N. (2022). The "Cerealization" of Continental North-West Europe, c.800–1200. In: *New Perspectives on the Medieval 'Agricultural Revolution': Crop, Stock and Furrow* (eds. McKerracher, M. & Hamerow, H.). Liverpool University Press, Liverpool, pp. 199–210.

Senn, C., Tinner, W., Felde, V.A., Gobet, E., van Leeuwen, J.F. & Morales-Molino, C. (2022). Modern pollen – vegetation – plant diversity relationships across large environmental gradients in northern Greece. *The Holocene*, 32, 159–173.

Seppä, H. & Bennett, K.D. (2003). Quaternary pollen analysis: recent progress in palaeoecology and palaeoclimatology. *Prog. Phys. Geogr.*, 27, 548–579.

Shakesby, R.A. (2011). Post-wildfire soil erosion in the Mediterranean: Review and future research directions. *Earth-Sci. Rev.*, 105, 71–100.

Simpson, G.L. (2024). gratia: An R package for exploring generalized additive models. *J. Open Source Softw.*, 9, 6962.

Spitzig, A., Rösch, M., Woodbridge, J., Bauch, M., Guzowski, P., Erhart, P., *et al.* (2025). Cultural innovation can increase and maintain biodiversity: A case study from medieval Europe. *Proc. Natl. Acad. Sci.*, 122, e2506266122.

Streifeneder, T., Giuliani, C. & Hoffmann, C. (2022). A cross-border analysis of the policies for Alpine pasture farming. In: *Cross-border spatial development in Bavaria – Dynamics in Cooperation – Potentials of Integration*. Verlag der AR, Hanover.

Sugita, S. (1994). Pollen Representation of Vegetation in Quaternary Sediments: Theory and Method in Patchy Vegetation. *J. Ecol.*, 82, 881–897.

Sugita, S. (2007). Theory of quantitative reconstruction of vegetation I: pollen from large sites REVEALS regional vegetation composition. *The Holocene*, 17, 229–241.

Sugita, S., Hicks, S. & Sormunen, H. (2010). Absolute pollen productivity and pollen–vegetation relationships in northern Finland. *J. Quat. Sci.*, 25, 724–736.

Thoen, E. (2018). Open Fields, Capital and Labour in Medieval and Early Modern Flanders. In: *Peasants and their Fields: The Rationale of Open-Field Agriculture, c.700–1800* (eds. Thoen, E., Williamson, T. & Dyer, C.). Brepols, Turnhout, pp. 163–182.

Väli, V., Odgaard, B.V., Väli, Ü. & Poska, A. (2022). Pollen richness: a reflection of vegetation diversity or pollen-specific parameters? *Veg. Hist. Archaeobotany*, 31, 611–622.

Van der Veen, M. (2016). Arable Farming, Horticulture, and Food: Expansion, Innovation, and Diversity. In: *The Oxford Handbook of Roman Britain*, Oxford Handbooks (eds. Millett, M., Revell, L. & Moore, A.). Oxford University Press, Oxford.

Verhulst, A. (2002). *The Carolingian Economy*. Cambridge University Press, Cambridge.

Vidaña, S.D. & Goring, S.J. (2023). neotoma2: An R package to access data from the Neotoma Paleoecology Database. *J. Open Source Softw.*, 8, 5561.

Ward-Perkins, B. (2005). *The Fall of Rome: And the End of Civilization*. Oxford University Press, Oxford.

Wickham, C. (2009). *The Inheritance of Rome: Illuminating the Dark Ages*. Penguin Books, New York.

Williams, J.W., Grimm, E.C., Blois, J.L., Charles, D.F., Davis, E.B., Goring, S.J., *et al.* (2018). The Neotoma Paleoecology Database, a multiproxy, international, community-curated data resource. *Quat. Res.*, 89, 156–177.

Wolf, A., Callaghan, T.V. & Larson, K. (2008). Future changes in vegetation and ecosystem function of the Barents Region. *Clim. Change*, 87, 51–73.

Wood, S.N. (2011). Fast stable restricted maximum likelihood and marginal likelihood estimation of semiparametric generalized linear models. *J. R. Stat. Soc. Ser. B Stat. Methodol.*, 73, 3–36.

Yeloff, D. & Van Geel, B. (2007). Abandonment of farmland and vegetation succession following the Eurasian plague pandemic of ad 1347–52. *J. Biogeogr.*, 34, 575–582.

Acknowledgments:

Data were obtained from the Neotoma Paleoecological Database (http://www.neotomadb.org) and its constituent databases, in particular the European Pollen Database and the Alpine Pollen Database. The work of data contributors, data stewards, and the Neotoma community is gratefully acknowledged. We thank David Orton and Rowan Mclaughlin for helpful discussions relating to the historical and archaeological context of the European High and Late Middle Ages. We thank Ben Powell and Marina Knight for helpful discussions regarding the statistical modelling. The Viking2 cluster was used during this project, which is a high-performance computing facility provided by the University of York. We are grateful for computational support from the University of York, IT Services and the Research IT team. Correspondence and requests for materials should be addressed to Jonathan D. Gordon. For the purpose of open access a Creative Commons Attribution (CC BY) licence is applied to any Author Accepted Manuscript version arising from this submission. This work was funded by a Leverhulme Trust Research Centre - The Leverhulme Centre for Anthropocene Biodiversity, grant number: RC-2018-021 (JDG, BF, JF, LG, NM, CDT all recipients).

Supporting Information

Extended Methods

Data availability

All pollen and chronological data used in this study are open access and obtained from the Neotoma Paleoecological Database (Williams *et al.* 2018) (hereafter 'Neotoma', accessed July 2024) and its constituent databases, in particular the European Pollen Database and the Alpine Pollen Database (Fyfe *et al.* 2009). *Supporting Information: Extended Figures and Tables, Extended Table 4* details the individual pollen records, and their locations, included in these analyses. Data used for the REVEALS steps can be found in Githumbi *et al.* (2022).

Code availability

We performed all data manipulations and analyses in this study in **R** (R Core Team 2022) and all 'packages' mentioned throughout are software extensions to **R**. Analysis code is available at: https://doi.org/10.5061/dryad.z08kprrrr.

Pollen data processing and standardisation

Data filter

We applied criteria relating to each pollen record's chronological and pollen sampling intensities to the total dataset downloaded from Neotoma (data downloaded July 2024). We included pollen records that contain two or more chronological control points (usually radiocarbon dates) from within the Common Era, each separated by no more than 1,000 years, and three or more Common Era pollen samples. Each of these pollen samples was required to contain a minimum number of terrestrial pollen grains (excluding spores), the details of which are discussed below (see *Pollen resampling*). If a specific section of any given pollen record conformed with these criteria, but the record as whole did not, we included that conforming section. If multiple sections of any given pollen record conformed with these inclusion criteria, but the record as a whole did not, we included the section with the most chronological control points (that also must satisfy the pollen sampling criteria). This ensured that each pollen record was included only once in our analyses.

Age-depth modelling

We constructed updated Bayesian age-depth models for all records that met our inclusion criteria using the package **`Bchron`** (Haslett & Parnell 2008). Given that all records included in these analyses are located in the northern hemisphere, we calibrated all radiocarbon dates using the IntCal20 calibration curve (Reimer *et al.* 2020). We ran each age-depth model for 40,000 iterations, with a thin value of 40, discarding the first 10,000 iterations. We did not allow extrapolated age estimates beyond 500 years from the outermost radiocarbon dates. We drew 1,000 age estimates per depth from each pollen record's posterior age distribution, and carried these forwards to the resampling stage. This sampling approach incorporates the uncertainty associated with age-depth modelling procedures and ensures

against spuriously confident age estimates (as would be achieved from simply taking the median age estimate per depth).

Modelling past vegetation covers from pollen counts

Fossil pollen data contain information relating to past vegetation communities. Despite this, pollen-vegetation relationships are non-linear and are affected by pollen source area (the relevant geographical area over which pollen is contributed to a record), relative differences in pollen production and dispersal between pollen producing plants, and taphonomy (i.e., between-pollen type and between-archive differences in pollen preservation in environmental archives) (Prentice 1985; Seppä & Bennett 2003; Sugita *et al.* 2010). Left unaccounted for, these factors have the capacity to strongly bias pollen diversity measures. For example, if a sample is dominated by a numerically dominant pollen type (e.g., from a high pollen producing plant or a well-dispersed pollen type) then the likelihood of sampling a pollen grain that does not belong to that pollen type is reduced, artificially depressing the apparent diversity of that pollen assemblage (Senn *et al.* 2022).

To overcome these biases (as far as is possible), we modelled pollen counts using the "Regional Estimates of VEgetation Abundance from Large Sites" (REVEALS) model (Sugita 2007), using the REVEALS model code from Abraham *et al.* (2014). The REVEALS model is a mechanistic model that takes pollen count data and a number of pollen-type and record-specific abiotic variables [which we obtained from Githumbi *et al.* (2022)] as input data, to provide proportional estimates (per pollen sample) of past vegetation covers [see Githumbi *et al.* (2022) for further detail of method] per pollen sample. Of the total set of pollen records available on Neotoma, 695 of them had the necessary data collected by Githumbi *et al.* (2022) to run the REVEALS model. Thus, for each of these 695 pollen records that also satisfied our data inclusion criteria (a total of 109 records), we ran the REVEALS model across all pollen samples in each record in turn. We then multiplied the original per-sample pollen counts by the outputted REVEALS proportional past vegetation estimates to convert

the REVEALS estimates back to pollen counts, following Felde *et al.* (2016). The REVEALS model provides past vegetation estimates for the most numerically abundant pollen types in fossil pollen spectra and we added the adjusted counts for these taxa back to the original dataset, carrying them forwards to the next stage of our analyses.

Pollen harmonisation

We harmonised the names of all pollen types present across our Common Era datasets using an updated European pollen harmonisation table (Birks *et al.* 2023) and summed the REVEALS-transformed counts by these names per sample.

Pollen resampling

These analyses include pollen data originating from 109 individual studies, the sum of which represent a wide range of methodological choices relating to pollen sampling and quantification. Thus, given the heterogeneity in pollen sampling intensities between pollen records, and the bias this would introduce to any computed diversity metrics if left unaccounted for (samples with more pollen grains counted are likely – on average – to have higher diversity estimates), we undertook a pollen resampling procedure to standardise counts across samples and records, resampling 150 grains from each sample using the `rrarefy` function from **`vegan`** (Oksanen *et al.* 2022).

REVEALS-transformed pollen counts represent original pollen sums multiplied by estimates of proportional past vegetation cover. These adjusted samples thus represent a dataset of pollen samples with total pollen sums often multiple factors lower than the original (i.e., non-REVEALS-transformed) counts. This is highlighted by *Supporting Information: Extended Figures and Tables, Extended Fig. 1F*, which shows the distribution of total terrestrial pollen sums across the 4,616 included pollen samples *before* they were adjusted by the vegetation estimates from REVEALS and underlines the high sampling intensity of the included

samples. To prevent the majority of samples (and therefore sites, see *Data filter*) being excluded, we chose 150 grains as the resample value, approximately in line with previous studies using a similar REVEALS methodology (e.g., Felde *et al.* 2016).

We repeated this resampling procedure 1,000 times. For each of these 1,000 random resamples, we added a random realisation from the posterior distribution of the relevant age-depth model to each sample (which relates to a level [depth] through the pollen sequence). We carried these 1,000 datasets forwards to the next stage of our analyses, thereby including the uncertainty inherent to the age-depth modelling and pollen resampling procedures in our analyses.

Pollen diversity and composition measures

In these analyses, we examine the effects on diversity of the major depopulation and cultural shifts that occurred across Europe during the 14th Century. This required a pollen dataset with pollen samples before and after the disturbances of the 14th Century. We thus filtered our total Common Era pollen dataset to include only records with pollen samples across the period of interest, filtering out those pollen records that did not have at least one pollen sample present in the 13th Century (1200 – 1300 CE) and the 15th Century (1400 – 1500 CE); i.e., spanning the 14th Century (see *Supporting Information: Extended Figures and Tables, Extended Fig. 1G* summaries of the numbers of samples present in the two time windows across the 109 records). Following the implementation of the criteria described in *Data filter,* the inclusion of only records with the requisite REVEALS information, the resampling procedure (exclusion of all samples with fewer than 150 grains) and the selection of only records with samples spanning the 14th Century, our final Common Era dataset included 109 unique pollen records constituted by 4616 unique REVEALS-adjusted pollen

samples spanning the period 0 – 1850 CE (*Supporting Information: Extended Figures and Tables, Extended Fig 1*).

For each of the 1,000 datasets, we computed the three measures of within-pollen record diversity: richness, evenness and compositional turnover (temporal beta diversity).

Richness and evenness

Richness represents the number of unique pollen types present in a standardised pollen sample (Birks & Line 1992); 150 grains in these analyses. Evenness is a measure of dominance, i.e., a measure of how a sample's total pollen sum is shared among pollen types. A pollen sample where the majority of pollen grains are identified as one or a few pollen types is considered 'uneven' (i.e., has low evenness values), whereas a pollen sample where the total pollen sum is shared more equally among pollen types is considered 'even' (high evenness values). We use Pielou's evenness (Pielou 1966) in these analyses, computed for each pollen sample using the **`vegan`** package (Oksanen *et al.* 2022).

Pollen richness is associated with the evenness of samples, such that strongly uneven samples are likely to have lower richness values than more even samples (Giesecke *et al.* 20a), a problem exacerbated by those confounding issues of differential pollen production, dispersal, preservation, etc., mentioned above (see *Modelling past vegetation covers from pollen counts*). We mitigate against these biases, as far as is possible, by adjusting pollen counts using REVEALS past vegetation estimates. Pollen richness has been shown to represent the richness of parent plant communities in European studies (e.g. Felde *et al.* 2016; Meltsov *et al.* 2011; Papadopoulou *et al.* 2022; Senn *et al.* 2022; Väli *et al.* 2022), though elsewhere this relationship does not always hold e.g., (Goring *et al.* 2013).

Compositional turnover (temporal beta diversity)

We computed the compositional turnover of pollen samples between successive samples through each pollen record using the Bray-Curtis index (Bray & Curtis 1957). Bray-Curtis accounts for differences in the abundances as well as identities of pollen types between samples, which we computed using the `vegdist` function from **`vegan`** (Oksanen *et al.* 2022). We adjusted for the time interval between successive samples in the same way as in Gordon *et al.* (2024). Briefly, this involved subtracting the expected difference in Bray-Curtis (given the time interval between samples) from the actual value, and normalising this value to be between [0,1] [see Gordon *et al.* (2024) for full details].

Agricultural land and tree cover

Alongside our pollen diversity metrics, we also analyse two metrics that describe changes to the composition of pollen samples: i) Agricultural land and ii) tree cover (Fig. 2). Table 1 in Githumbi *et al.* (2022) describes the land cover classes (LCCs) and plant functional types (PFT) used by Wolf *et al.* (2008) to group together vegetation estimates from different pollen types. We implement the methodology from Githumbi *et al.* (2022) for our REVEALS pollen count transformation stage and we group the resultant vegetation estimates using the same LCC and PFT groups. Our tree cover group comprises all pollen types included in the 'Evergreen trees' LCC and 'Summer-green trees' LCC, whilst our Agricultural land group contains pollen counts from the pollen types Cerealia t. and *Secale cereale*, and is identical to the PFT of the same name in Table 1 of Githumbi *et al.* (2022).

Fourteenth Century agricultural land trajectory

To understand how changes in cereal cultivation related to changes in each diversity metric, we subset pollen records into three categories based on their changing cereal pollen representation across the 14th Century. For each resampled pollen record (1,000 resamples per record), we first computed the mean cereal count of all pollen samples that fell into time

period one, 1200 – 1300 CE, and for all pollen samples that fell into time period two, 1400 – 1500 CE (such that each pollen record was represented by an average cereal count value for both periods). We then computed the difference between these two average cereal count values to provide the 'trajectory' of change over the 14th Century for that resampled pollen record. We categorised these change values into (i) 'cereal farming continuation/expansion'; pollen records that had non-zero cereal counts and that remained the same/showed increases in cereal cultivation, (ii) 'cereal farming abandonment'; pollen records that showed decreases in cereal cultivation and (iii) 'non-cereal farming locations'; pollen records that had zero cereal pollen represented in both the 1200 – 1300 CE period and the 1400 – 1500 CE period. We repeated this categorisation procedure for all 1,000 resamples of each pollen record and carried through to the modelling stage (described below).

It is worth noting that the reduction of REVEALS-transformed cereal counts in a pollen record is most plausibly a consequence of reduced areal coverage of cereal crops, in some cases to zero (8.9% of resampled records showing declines to zero) and in other cases to a lower level (median reduction for resampled records where cereal prevalence reduced = 64.1% decline, 25th quantile = 100% decline, 75th quantile = 33.3% decline). Reduced intensity in a similar area cultivated is theoretically possible, but less likely because of the large effort required to cultivate land in pre-industrial agricultural systems.

Temporal trends

Given our large Common Era dataset (n = ~5,000 unique pollen samples x 1,000 resamples) and the computational expense of fitting Generalised Additive Models with many thousands of parameters (smooths and random effects), it was computationally intractable to model the total dataset of 1,000 resamples per diversity metric through time in a single model. To

overcome this, we employed a bootstrapping and posterior simulation procedure to ensure that the variation across all 1,000 resampled diversity metrics and their per-sample age-distributions, alongside statistical uncertainty associated with model fitting, was carried through these analyses.

To ensure computational feasibility, we subset the total dataset of 1,000 resamples per metric into ten blocks, with each block containing 100 unique resamples. For each block of 100 resamples per pollen metric (richness, evenness, turnover, agricultural land), we fit a Generalised Additive Model to:

1. The full dataset, i.e., a Europe-scale analysis (Figs. 1A-D)
2. The full dataset, subset by 14th Century cereal trajectory (Figs. 1E-H)
3. The full dataset subset (spatially) by each vegetation zone (Lang *et al.* 2023) (Figs. 4A-C).

For each metric, block and spatial subset of the data (1-3, above) combination (`Metric_i`, below), we fit a GAM to the pollen data as a function of time and a random intercept term for each unique dataset ID. These models took the form,

```
Metric_i ~ s(age_CE, by = "resample", bs = "fs") +
           s(datasetid, bs = "re"),
         discrete = T,
         method = "fREML",
         nthreads = 50,
         family = fam.
```

We chose the Poisson family for the richness models (given the count response) and the beta family for the evenness and turnover models (given the [0, 1] constraints of the data).

We chose the negative binomial family for the Agricultural land models, given the overdispersed nature of the count response. We discretized all variables and fit these models using fast restricted maximum likelihood (fREML) and `bam` to speed up model fitting (Wood 2011). We performed model checks by inspecting histograms of residuals and residuals versus fitted plots, which did not show any patterns and were thus deemed acceptable. We also checked the outputs from **mgcv**'s `gam.check` function to ensure that all models had converged and that the wiggliness provided for each smooth (*k*) was sufficient.

We combined the fitted smooths across the ten blocks per metric and spatial unit using a posterior simulation approach. For each model fit, we simulated 100 draws from the posterior of each estimated function using the `fitted_samples` function from **`gratia`** (Simpson 2024). Given the estimated model parameters, this function generates posterior draws (i.e., realisations) for each fitted function to include the uncertainty in the expected values. This posterior simulation procedure resulted in 100 draws associated with each of the 1,000 (original) resamples, which resulted in 100,000 individual draws for each metric, spatial unit (Europe/vegetation zone) and cereal trajectory combination through time across the total dataset. We summarise and present these 100,000 draws using the median and a 90% credible interval for each metric (Fig. 1, Fig 4A-C and *Supporting Information: Extended Figures and Tables, Extended Fig. 2*).

To quantify the rate of change (and subsequently check if they are predominantly positive or negative) through each draw, d, of each metric, m, for each spatial type, s, and cereal trajectory type, c, we approximated the first derivative (slope) of m, m', using the method of central finite differences. That is,

$$m'_{d,s,c}(t) \approx \frac{m_{d,s,c}(t+h) - m_{d,s,c}(t-h)}{2h},$$

i.e., the change in the metric between the next time point and the previous time point divided by the total amount of time between the two time points. Here, h is the gap between two time points and is set to be two, as the predictions are made across an evenly spaced grid at an interval of two years over the Common Era.

We performed this procedure for each of the 100,000 temporal smooths per diversity metric, spatial unit and cereal trajectory combination, which provided a distribution of derivative estimates over the Common Era. We plot in bold time points for which 95% of the estimates were either positive or negative (bold used for both), which provides a level of confidence in the modelled temporal changes. We plot all the other time points in non-bold (Figs 1 & 4).

Relationships between metrics

The analyses described below included pollen samples from within the time period 1200 – 1300 CE only and thus included orders of magnitude fewer pollen samples than were analysed in the procedures outlined in *Temporal trends* (above). Given the substantially lower computational requirements to fit these models, for the following analyses we were able to model the full dataset (i.e., all 1,000 resamples) in the *same* model (i.e., one GAM of 1,000 resampled datasets vs ten GAMs that each contained 100 resamples as in *Temporal trends*). We performed the following analyses for the full European dataset (Fig. 3) and for each vegetation zone (Fig. 4D-I).

<u>Diversity and tree cover</u>

Our expectation was that diversity values should be maximised in landscapes characterised by approximately balanced levels of open versus wooded cover. To investigate this expectation, we modelled i) how tree cover related to richness and, using predictions from

this model, ii) how tree cover change related to richness change spanning the 14th Century. We firstly subset all pollen records that were represented by pollen samples spanning the Black Death era (samples present in both the period 1200 – 1300 CE and 1400 – 1500 CE). We then modelled the richness data as a function of tree cover for those pollen samples that fell into the period 1200 – 1300 CE. We had no *a priori* expectation for the 'best fitting' functional form of tree cover, so we used a GAM to estimate this (potentially smooth) relationship. This model took the form,

```
richness ~ s(tree_percent, bs = "tp",
               k = 7, m = 2) +
             s(datasetid, bs = "re") +
             s(tree_percent, resample,
               bs = "fs", k = 5, m = 2),
         method = "fREML",
         discrete = T,
         nthreads = 10,
         family = poisson.
```

We included a random intercept term for each unique pollen record. We also allowed the functional form for the effect of tree cover on richness to vary by resample. The argument `bs = "fs"` selects the factor-smooth interaction basis type and `m = 2` penalises the spline (preventing overly wiggly forms) using the second derivative of the function. See Pedersen *et al.* (2019) for further details of fitting hierarchical generalised additive models using **mgcv** in **R**. We chose the Poisson distribution as the family, given the count response. Again, we discretized all variables and fit these models using fast restricted maximum likelihood (fREML) and `bam` to speed up model fitting (Wood 2011).

We performed the same model checks as for the temporal models and present the fit of the global `tree_percent` smooth, plus the data and prediction uncertainty for individual records across the 1,000 resamples, in Figs. 3A for Europe and in Figs. 4D-F for each vegetation zone.

According to our hypothesis, a reduction in tree cover in landscapes dominated by trees would generate biodiversity gains, whereas in landscapes largely devoid of trees, further reductions in tree cover would erode diversity measures (and *vice versa*). Using the above model trained using the 13th Century data only, we predicted the expected (temporal) change in richness given the actual changes in tree cover between the 13th and 15th Centuries (for each resample). This prediction provided the expected change in richness between the 13th and 15th Centuries for each pollen record, given the estimated smooth relationship between richness and tree cover presented in Fig. 3A. We also computed the change in the raw (observed) richness data for each pollen record over the same time period.

To identify how well the modelled expectation related to the actual changes observed, we fitted a linear model to the observed change in richness (`delta_observed_richness`, below) as a function of the predicted change in richness (`delta_predicted_richness`) across the 1,000 resamples, (Fig. 3B). This model took the form,

```
Delta_observed_richness ~ delta_predicted_richness +
                          s(datasetid, bs = "re") +
                          s(resample,
                          delta_predicted_richness, bs = "re"),
                method = "fREML",
                discrete = T,
```

```
                    nthreads = 10,
                    family = gaussian
```

We chose the Gaussian family for this model, given the continuous, zero-centred response. We also included a random intercept term for each unique pollen record and a random slope and intercept for each resample. Again, we discretized all variables and fit these models using fast restricted maximum likelihood (fREML) and `bam` to speed up model fitting (Wood 2011).

We present the overall relationship between changes in predicted and observed richness, plus the data and prediction uncertainty across the 1,000 resamples for Europe in Fig. 3B and for each vegetation zone in Fig. 4G-I.

Diversity and cereals

We also were interested in how richness and evenness related to cereal representation in the period immediately before the Black Death. We subset pollen records with samples spanning the Black Death era, i.e., with samples in both the 1200 – 1300 CE and 1400 – 1500 CE time periods (in the same way as for the *Diversity and tree cover* models; see above). The distribution of raw cereal counts were heavily right skewed, with a high proportion of zeros and we therefore square-root transformed them. Then, we fit a GAM to the 1200 – 1300 CE diversity data (richness and evenness, `Diversity` below), with a smooth function of square-root transformed cereal counts as the explanatory variable. These models took the form,

```
    Diversity ~ s(sqrtcereal, bs = "tp", k = 10, m = 2) +
                s(sqrtcereal, resample, bs = "fs",
                  k = 5, m = 2),
```

```
            method = "fREML",
            discrete = T,
            nthreads = 10,
            family = fam.
```

We chose the Poisson family for the richness model (given the count response) and the beta family for the evenness model (given the [0, 1] constraints of the data). Again, we allowed the functional form and intercepts for the effect of `sqrtcereal` on `Diversity` to vary by resample. We did not include a random intercept for each unique dataset ID, as in the tree cover model, because it prevented convergence when included. We present the fit from the global smooth plus the data and prediction uncertainty across the 1,000 resamples, in *Supporting Information: Extended Figures and Tables, Extended Fig. 3*.

Extended methods references

Abraham, V., Oušková, V. & Kuneš, P. (2014). Present-Day Vegetation Helps Quantifying Past Land Cover in Selected Regions of the Czech Republic. *PLOS ONE*, 9, e100117.

Birks, H.J.B., Bhatta, K.P., Felde, V.A., Flantua, S.G.A., Mottl, O., Haberle, S.G., *et al.* (2023). Approaches to pollen taxonomic harmonisation in Quaternary palynology. *Rev. Palaeobot. Palynol.*, 319, 104989.

Birks, H.J.B. & Line, J.M. (1992). The use of Rarefaction Analysis for Estimating Palynological Richness from Quaternary Pollen-Analytical Data. *The Holocene*, 2, 1–10.

Bray, J.R. & Curtis, J.T. (1957). An Ordination of the Upland Forest Communities of Southern Wisconsin. *Ecol. Monogr.*, 27, 325–349.

Felde, V.A., Peglar, S.M., Bjune, A.E., Grytnes, J.-A. & Birks, H.J.B. (2016). Modern pollen–plant richness and diversity relationships exist along a vegetational gradient in southern Norway. *The Holocene*, 26, 163–175.

Fyfe, R.M., de Beaulieu, J.-L., Binney, H., Bradshaw, R.H.W., Brewer, S., Le Flao, A., *et al.* (2009). The European Pollen Database: past efforts and current activities. *Veg. Hist. Archaeobotany*, 18, 417–424.

Giesecke, T., Ammann, B. & Brande, A. (2014). Palynological richness and evenness: Insights from the taxa accumulation curve. *Veg. Hist. Archaeobotany*, 23, 217–228.

Githumbi, E., Fyfe, R., Gaillard, M.-J., Trondman, A.-K., Mazier, F., Nielsen, A.-B., *et al.* (2022). European pollen-based REVEALS land-cover reconstructions for the Holocene: methodology, mapping and potentials. *Earth Syst. Sci. Data*, 14, 1581–1619.

Gordon, J.D., Fagan, B., Milner, N. & Thomas, C.D. (2024). Floristic diversity and its relationships with human land use varied regionally during the Holocene. *Nat. Ecol. Evol.*, 8, 1459–1471.

Goring, S., Lacourse, T., Pellatt, M.G. & Mathewes, R.W. (2013). Pollen assemblage richness does not reflect regional plant species richness: a cautionary tale. *J. Ecol.*, 101, 1137–1145.

Haslett, J. & Parnell, A. (2008). A simple monotone process with application to radiocarbon-dated depth chronologies. *J. R. Stat. Soc. Ser. C Appl. Stat.*, 57, 399–418.

Lang, G., Tinner, W., Morales-Molino, C., Schwörer, C. & Ammann, B. (2023). Late-glacial and Holocene vegetation changes and their causes. In: *Quaternary vegetation dynamics of Europe* (eds. Lang, G., Ammann, B., Behre, K.-E. & Tinner, W.). Haupt Verlag, Bern.

Meltsov, V., Poska, A., Odgaard, B.V., Sammul, M. & Kull, T. (2011). Palynological richness and pollen sample evenness in relation to local floristic diversity in southern Estonia. *Rev. Palaeobot. Palynol.*, 166, 344–351.

Oksanen, J., Simpson, G.L., Blanchet, F.G., Kindt, R., Legendre, P., Minchin, P.R., *et al.* (2022). *_vegan: Community Ecology Package_. R package version 2.6-2, \textlesshttps://CRAN.R-project.org/package=vegan\textgreater.*

Papadopoulou, M., Tsiripidis, I., Panajiotidis, S., Fotiadis, G., Veres, D., Magyari, E., *et al.* (2022). Testing the potential of pollen assemblages to capture composition, diversity and ecological gradients of surrounding vegetation in two biogeographical regions of southeastern Europe. *Veg. Hist. Archaeobotany*, 31, 1–15.

Pedersen, E.J., Miller, D.L., Simpson, G.L. & Ross, N. (2019). Hierarchical generalized additive models in ecology: An introduction with mgcv. *PeerJ*, 2019, e6876–e6876.

Pielou, E.C. (1966). The measurement of diversity in different types of biological collections. *J. Theor. Biol.*, 13, 131–144.

Prentice, I.C. (1985). Pollen representation, source area, and basin size: Toward a unified theory of pollen analysis. *Quat. Res.*, 23, 76–86.

R Core Team. (2022). *R: A Language and Environment for Statistical Computing*. R Foundation for Statistical Computing, Vienna, Austria.

Reimer, P.J., Austin, W.E.N., Bard, E., Bayliss, A., Blackwell, P.G., Ramsey, C.B., *et al.* (2020). The IntCal20 Northern Hemisphere Radiocarbon Age Calibration Curve (0–55 cal kBP). *Radiocarbon*, 62, 725–757.

Senn, C., Tinner, W., Felde, V.A., Gobet, E., van Leeuwen, J.F. & Morales-Molino, C. (2022). Modern pollen – vegetation – plant diversity relationships across large environmental gradients in northern Greece. *The Holocene*, 32, 159–173.

Seppä, H. & Bennett, K.D. (2003). Quaternary pollen analysis: recent progress in palaeoecology and palaeoclimatology. *Prog. Phys. Geogr.*, 27, 548–579.

Simpson, G.L. (2024). gratia: An R package for exploring generalized additive models. *J. Open Source Softw.*, 9, 6962.

Sugita, S. (2007). Theory of quantitative reconstruction of vegetation I: pollen from large sites REVEALS regional vegetation composition. *The Holocene*, 17, 229–241.

Sugita, S., Hicks, S. & Sormunen, H. (2010). Absolute pollen productivity and pollen–vegetation relationships in northern Finland. *J. Quat. Sci.*, 25, 724–736.

Väli, V., Odgaard, B.V., Väli, Ü. & Poska, A. (2022). Pollen richness: a reflection of vegetation diversity or pollen-specific parameters? *Veg. Hist. Archaeobotany*, 31, 611–622.

Williams, J.W., Grimm, E.C., Blois, J.L., Charles, D.F., Davis, E.B., Goring, S.J., *et al.* (2018). The Neotoma Paleoecology Database, a multiproxy, international, community-curated data resource. *Quat. Res.*, 89, 156–177.

Wolf, A., Callaghan, T.V. & Larson, K. (2008). Future changes in vegetation and ecosystem function of the Barents Region. *Clim. Change*, 87, 51–73.

Wood, S.N. (2011). Fast stable restricted maximum likelihood and marginal likelihood estimation of semiparametric generalized linear models. *J. R. Stat. Soc. Ser. B Stat. Methodol.*, 73, 3–36.

Extended Figures and Tables

Extended Figure 1. Fossil pollen record data descriptions. (A) Map describing locations of fossil pollen records (N = 109) included in these analyses, with the size of the icon representing the number of resamples (maximum 1,000) each pollen record is present in (given variation arising from probabilistic age modelling procedure). **(B)** The number of unique pollen records present in 100-year bins through the Common Era. **(C)** The number of unique pollen samples (N = 4,616) present in 100-year bins through the Common Era. **(D)** The number of unique samples per record in 100-year bins through the Common Era. Central orange points represent the median numbers of samples per record across all records present in each bin plus the 90% empirical interval (across records) around the mean, represented by the grey bar. The dotted line represents the median across bins. **(E)** The temporal coverage of each pollen record; each line represents one of the 109 records, cohort ordered by age and duration. **(F)** The terrestrial pollen sums of all 4,616 pollen samples included in these analyses prior to the REVEALS adjustment step. **(G)** The number of pollen samples in the time window prior to the Black Death era (1200 – 1300 CE) and after the Black death era (1400 – 1500 CE) across the 109 records included in these analyses. Pollen samples in panels **(B - E & G)** are temporally partitioned based on their median age across all 1,000 age draws from the posterior age distribution per sample. Note the logarithmic y-axes for panels **(D, F & G)**. The mean and standard error-based 95% confidence interval of the mean is shown as a yellow diamond and interval in panels **(F & G) -** note that the 95% interval is equal in size to the mean symbol in **(F)** so is not visible**.**

Extended Figure 2. Per-vegetation zone temporal patterns in each pollen metric. (A-C) Evenness, **(D-F)** turnover and **(G-I)** cereals. Generalised additive models fit to each metric as a smooth function of time. Central lines represent the average fit across the fitted distribution (see *Methods*), with sections of thicker lines indicating periods over which >95% of the temporal draws exhibit positive or negative slopes. Grey intervals represent the interquartile range across draws. Vertical black dotted lines show the bounds of the 14th Century.

Lack of 'significance' (thicker lines) for Mediterranean trends for richness (Fig. 4C), evenness and turnover reflects smaller sample sizes for this vegetation zone, given the reduced availability of pollen records for drier environments. Nonetheless, increased apparent values around 0 CE may reflect positive influences of earlier Mediterranean cultures on all three biodiversity metrics. It is unclear whether the growth of biodiversity metrics in the Boreal and Hemiboreal (Fig. 4A, panels A, D here) indicates limited impact of the Great Famine and Black Death and social-political changes (continuation of previous growth), or whether increases are directly linked to population relocation.

Extended Figure 3. Cereal representation and diversity relationships. (A) Richness and **(B)** evenness as nonlinear functions of cereal counts for pollen samples in the period 1200 – 1300 CE for Europe. In both panels, the central points represent the median and the crosshairs represent the variation (25th and 75th percentiles) across the 1,000 resamples in both diversity (richness and evenness) and cereal counts.

Extended Table 1. Model summaries, Fig. 3. Sheet 1: Tree cover and richness relationship, from Fig. 3A. Sheet 2: Change in predicted and change in observed richness relationship, from Fig. 3B. Parameter estimates and fitness estimates.

Extended Table 2. Model summaries, Fig. 4D-F. Per-vegetation zone tree cover and richness relationships, from Figs. 4D-F. Parameter estimates and fitness estimates.

Extended Table 3. Model summaries, Fig. 4G-I. Per-vegetation zone change in predicted and change in observed richness relationships, from Figs. 4G-I. Parameter estimates and fitness estimates.

Extended Table 4. Metadata for fossil pollen records included in these analyses. Columns: Sitename (unique site name), datasetid (unique Neotoma identifier per pollen record), collunitid (unique Neotoma collection unit identifier detailing pollen record origin), n_samples (number of pollen samples per record), n_chroncontrols (number of chronological controls per record), long (longitude in DD), lat (latitude in DD), citation (author names and DOI for original publication).